Single Mode ZnO Whispering-Gallery Submicron Cavity and Graphene Improved Lasing Performance

Jitao Li,[†,‡,§] Yi Lin,[†] Junfeng Lu,[†,§] Chunxiang Xu,[*,†] Yueyue Wang,[†] Zengliang Shi,[†] and Jun Dai[†]

[†]State Key Laboratory of Bioelectronics, School of Biological Science and Medical Engineering, Southeast University, Nanjing 210096, China and [‡]School of Physics and Electromechanical Engineering, Zhoukou Normal University, Zhoukou 466001, China. [§]J. Li and J. Lu contributed equally to this work.

ABSTRACT

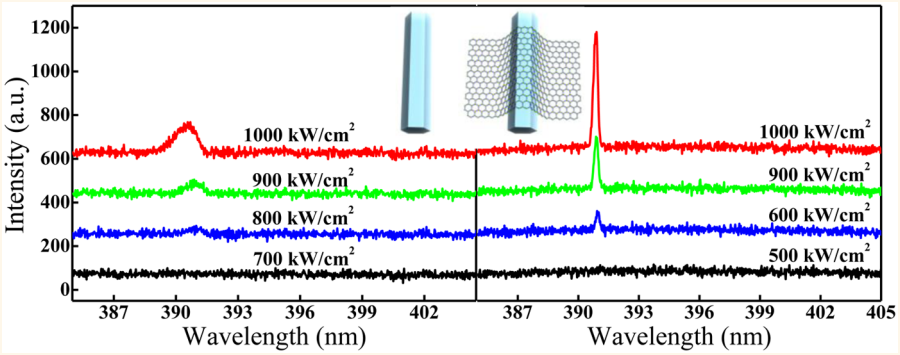

Single-mode ultraviolet (UV) laser of ZnO is still in challenge so far, although it has been paid great attention along the past decades. In this work, single-mode lasing resonance was realized in a submicron-sized ZnO rod based on serially varying the dimension of the whispering-gallery mode (WGM) cavities. The lasing performance, such as the lasing quality factor (*Q*) and the lasing intensity, was remarkably improved by facilely covering monolayer graphene on the ZnO submicron-rod. The mode structure evolution from multimodes to single-mode was investigated systematically based on the total internal-wall reflection of the ZnO microcavities. Graphene-induced optical field confinement and lasing emission enhancement were revealed, indicating an energy coupling between graphene SP and ZnO exciton emission. This result demonstrated the response of graphene in the UV wavelength region and extended its potential applications besides many previous reports on the multifunctional graphene/semiconductor hybrid materials and devices in advanced electronics and optoelectronics areas.

KEYWORDS: ZnO · single-mode lasing · whispering-gallery mode · graphene · submicron-cavity

The wide direct band gap (3.37 eV) and strong exciton binding energy (60 meV) of ZnO have drawn people's great endeavor to explore the short-wavelength lasers and their potential applications in recent decades.[1−3] So far, ultraviolet (UV) lasing of ZnO has been carried out in different resonant cavities of random, Fabry−Perot (F−P), and whispering-gallery mode (WGM).[4−6] Among them, WGM lasing has attracted intensive interest due to its high quality factor (*Q*) and low lasing threshold based on the total internal-wall reflection of the microcavity.[6,7] All reported WGM lasing just presented multimode structure in micron-sized ZnO cavities with sufficient gain.[6,8,9] However, high performance UV lasers with good monochromaticity, *i.e.*, single-mode lasing with narrow spectral line width, are much desirable for practical applications,[10] such as optoelectronic integration, micro-spectroscopy photometers and ultrasensitive chemical/biological sensors.

A general approach to achieve single-mode lasing is designing and fabricating the multilayered films or gratings with distributed Bragg reflection (DBR) or distributed feedback (DFB) structures.[11−13] Another way is to select a common mode from two coupled cavities by means of Vernier effect.[14−16] For example, Shang *et al.* realized a directional single-mode lasing in a coupled asymmetric microcavity by coupling two size-mismatched circular resonators.[17] However,

* Address correspondence to xcxseu@seu.edu.cn.

Received for review October 21, 2014 and accepted July 4, 2015.

Published online July 04, 2015
10.1021/acsnano.5b01319

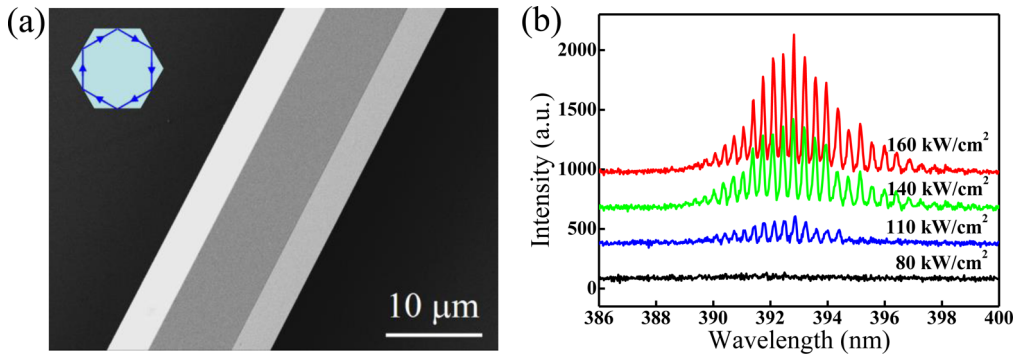

Figure 1. (a) SEM image of an individual hexagonal ZnO microrod. The top-left inset shows schematic of a WGM resonant cavity of the microrod and the light propagation path. (b) Excitation power density dependent PL spectra of the ZnO microrod.

these two approaches rely on sophisticated fabrication techniques and high cost. The third one, a fairly optional strategy to achieve the single-mode lasing, is reducing the resonator size to make the free spectral range (FSR) of a cavity exceed the spectral width of the gain medium.[18,19] As a representative report, Gargas *et al.* obtained single-mode ZnO WGM lasing from individual ZnO nanodisk with diameter of several hundred nanometers.[19] Unfortunately, the drastically increased optical loss is unavoidable as the cavity size is reduced.[20] Facing to this problem, the extreme light-matter interaction is expected to carry out through plasmon coupling in semiconductor laser, which combines the sufficient gain of semiconductor and spatial electromagnetic field confinement of surface plasmon (SP). This provides a promising way to construct a nanoscaled lasing cavity. Until now, various plasmonic nanolasers have been attempted in bimetallic porous nanowires,[21] nanopatch,[22] nanodisks,[23] coaxial and ring structures.[24,25] For example, Li *et al.* reported single-mode WGM lasing realized in a hexagonal GaN nanopillar array with pillar diameter of about 980 nm.[18] The most important role in their realization is the metal cladding layer, which promotes optical confinement within the cylindrical cavity. Oulton *et al.* reported a nanometer-scale plasmonic laser in a high-gain CdS nanowire on top of a silver substrate spaced with a thin MgF_2 layer.[26] Owing to the strong mode confinement, the spontaneous emission rate was accelerated dramatically and the stimulated emission generated optical modes one hundred times smaller than the diffraction limit. However, the metal SP is inconveniently tunable in fixed devices and generally has large Ohmic loss,[27,28] which hinders the flexible design and development of novel functional photonic materials and devices with high performance.

Fortunately, graphene, a flat two-dimensional monolayer composed of carbon atoms, has been considered as a plasmonic material alternative to noble metals based on its unique conductivity and optical properties.[29,30] Graphene SP has been employed to strengthen the light-matter interaction[31,32] and adopted to enhance the spontaneous and stimulated emission of ZnO.[33−35] Though many reports have demonstrated the PL enhancement from graphene-coated ZnO and assumed the action of graphene SP, the mechanism is unclear; especially, the understanding of the response of graphene SP in UV region is in some controversy.[36] Direct evidence of the important characteristics of graphene SP, such as the field spatial confinement and the corresponding optical field enhancement, is still scarce in experiment.

In this work, an easily accessible approach to achieve single-mode lasing of ZnO was proposed and realized in a submicron-sized ZnO cavity based on the systematic investigation on the WGM lasing behaviors of ZnO microrods with different diameters. More importantly, the single-mode lasing performance was remarkably improved by facilely covering monolayer graphene on the ZnO rod to construct a graphene/ZnO hybrid submicron-cavity, in which the optical field was effectively confined and the optical gain was sufficiently elevated based on the graphene SP coupling with ZnO exciton emission.

RESULTS AND DISCUSSION

In order to investigate the optical behaviors of the bare ZnO microrods, a typical microrod with diameter of $D = 15.5\ \mu$m, as shown the SEM image in Figure 1a, was selected individually. The microrod exhibits a perfect hexagonal cross-section and flat and smooth side surfaces, so the light can be well confined and propagate circularly in the cavity to form WGM resonance due to the multiple total internal-wall reflection at the ZnO/air interfaces, as schematically shown in the inset of Figure 1a. Figure 1b shows the excitation power density dependent PL spectra of the microrod. At a low excitation power density of 80 kW/cm^2, the PL spectrum presents a broad spontaneous emission, which comes from the near band-edge (NBE) emission of ZnO.[37] When the excitation increased to 110 kW/cm^2, the PL intensity increased and some sharp peaks appeared in the spectrum, indicating the lasing generation in the microcavity. Under more higher

excitation of 140−160 kW/cm^2, more sharp and stronger lasing peaks emerged in the spectra. For a typical lasing mode at wavelength of 392.7 nm, the full width at half-maximum (fwhm) is about 0.08 nm, so the Q factor is calculated as about 4900 according to the equation $Q = \lambda/\delta\lambda$, where λ and $\delta\lambda$ are the lasing mode wavelength and its fwhm, respectively. The experimental mode spacing matches well with the calculated value according to the equation of mode spacing for a WGM cavity:

$$\Delta\lambda = \lambda^2/[L(n - \lambda dn/d\lambda)] \quad (1)$$

where L is the path length of a round trip, n is the refractive index of ZnO, and $(dn/d\lambda)$ denotes the dispersion relation. On the other hand, the mode structure at excitation power density of 160 kW/cm^2 was also numerically calculated according to the WGM lasing equation

$$N = \frac{3\sqrt{3}nD}{2\lambda} - \frac{6}{\pi}\tan^{-1}h\sqrt{3n^2 - 4} \quad (2)$$

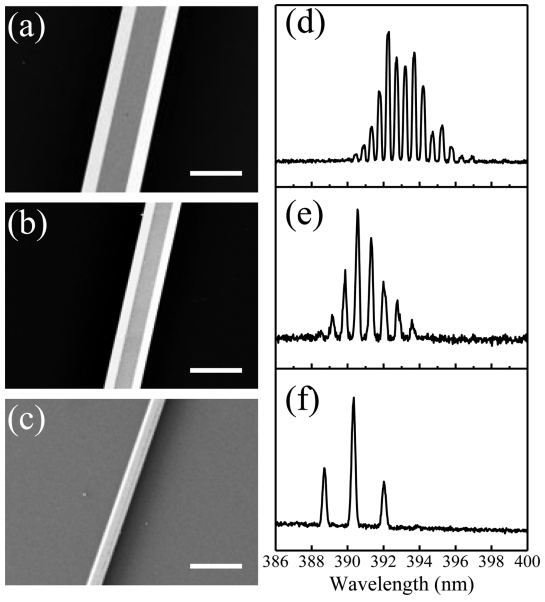

Figure 2. SEM images and corresponding lasing spectra of the ZnO microrods with different diameter of (a) 11.9, (b) 6.9 and (c) 2.8 μm, respectively. The scale bar is 10 μm.

where N is the mode number, n is the refractive index of ZnO, D is the diameter of the microrod. The calculated modes match with the experimentally observed lasing peak positions very well. So we can conclude definitely that the lasing emission from the ZnO microrod is attributed to the WGM lasing mechanism.

To get more information about the WGM lasing from the ZnO microrods, the size-dependent lasing characteristics were further systematically investigated by varying diameter of the ZnO microrods ranging from 15.5 to 2.8 μm. Figure 2a−f show SEM images and corresponding lasing spectra of three representative ZnO microrods with diameter of 11.9, 6.9, and 2.8 μm under the same excitation condition. From the lasing spectra shown in Figure 2d−f, one can see clearly that the number of the resonant mode decreases with size reduction of the microrod, such that there are only three resonant modes for the ZnO microrod with diameter of 2.8 μm. Only one resonant mode (*i.e.*, single-mode resonance) appearing in the spectrum is speculated naturally if diameter of a ZnO microrod is reduced to a dimension small enough to make the FSR of the cavity exceed the spectral width of the gain medium.[19,38,39] It is also found that the fwhm and mode spacing of the lasing modes increase with decreasing of the microrod diameter. The broad fwhm means the low Q factor of the small microcavity due to the optical loss increases with decreasing of the cavity diameter. Meanwhile, the wider mode spacing of the microcavity with smaller diameter agrees well with the theoretical prediction of eq 1.

As discussed above, a microrod with smaller diameter has less resonant modes than a bigger one has. Interestingly, a single-mode resonance was observed in a submicron-sized ZnO rod. As shown the SEM image in Figure 3a, the submicron-sized ZnO rod exhibits regular hexagonal cross-section with diameter of about 600 nm and smooth side surfaces. Figure 3b shows the PL spectra of this rod under different excitation power densities. Only one resonant peak appears at wavelength of 390.5 nm, and the lasing threshold is about 800 kW/cm^2. The fwhm of the lasing

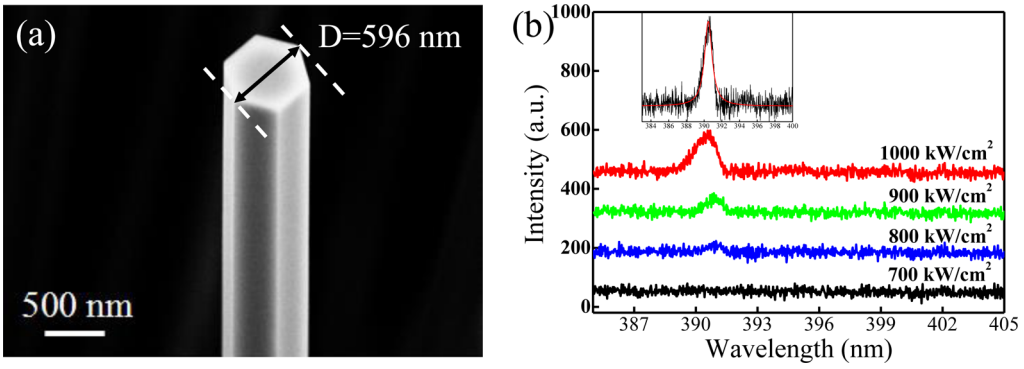

Figure 3. (a) SEM image of a submicron-sized ZnO rod. (b) Excitation power density dependent PL spectra of this rod. The inset in (b) shows Lorentzian fitting (red line) of the PL spectra at excitation power density of 1000 kW/cm^2.

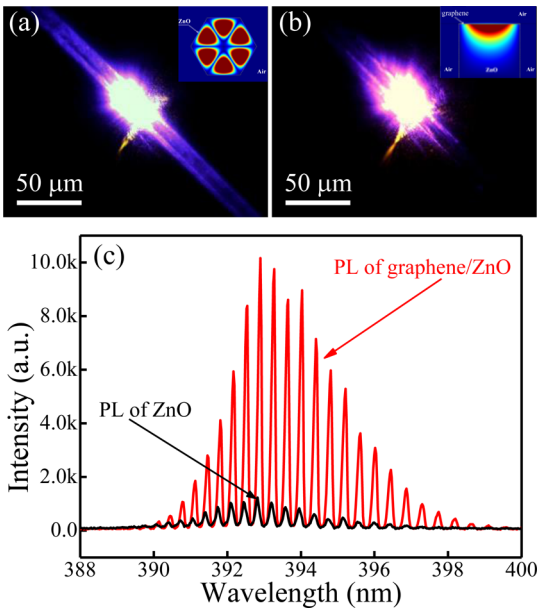

Figure 4. Dark field optical images of an individual ZnO microrod (a) before and (b) after being covered with graphene under the same excitation condition. The inset in (a) and (b) shows electric field energy distribution in the cross-section plane of the bare ZnO microrod and the evanescent field distribution of the 1st order eigenmode of graphene SP in the interface of air/graphene/ZnO, respectively. (c) Comparison of the PL spectra from the same ZnO microrod before (black line) and after (red line) graphene covering under the same excitation condition of 160 kW/cm^2.

peak is collected as about 0.98 nm from the inserted Lorentzian fitting of the spectrum at excitation power density of 1000 kW/cm^2, so the Q factor is calculated as about 400 according to the equation, $Q = \lambda/\delta\lambda$. This Q value is much lower than those of the microrods shown in Figure 1 and 2, because the Q factor of a traditional dielectric microcavity decreases drastically due to the more radiation loss in a smaller cavity,[20] which also presented higher lasing threshold than its counterparts of the bigger sized microrods discussed above.

Experimentally, an obvious optical field confinement was observed after the microrod was covered with graphene. Figure 4a and b compare the optical images of the same ZnO microrod before and after graphene covering under the same excitation condition. In Figure 4a, the bare ZnO microrod emits bright light under the UV excitation, meanwhile, a part of the emission propagates along the microrod and leaks out from the excitation spot, which causes proper radiation loss for resonance. While after the microrod was covered with graphene, the graphene/ZnO hybrid microcavity emits much brighter dazzling light under the same excitation condition, as shown in Figure 4b. It is very interesting to note that the emission light was almost confined in the excitation spot, which is quite different from the propagation and attenuation phenomena observed in the bare microcavity. The spatial confinement of the optical field just fits the typical characteristic of SP. Previously, Nair and Sun *et al.* have demonstrated the abnormal UV absorption of graphene,[40,41] which implied the SP generation in short wavelength region due to the oscillation of π electrons. In present case, the effective optical field confinement is ascribed to the sufficient electromagnetic field overlap between the resonant optical field of ZnO and graphene SP wave. In principle, the resonant optical field of ZnO mainly distributes near the WGM cavity surface based on the total internal-wall reflection (inset in Figure 4a), while graphene SP as an evanescent wave is also highly localized near the surface. When top surface of the ZnO microrod was covered with graphene, it is noted that the graphene SP mainly distributed in the ZnO side near the covered graphene, as shown the inset in Figure 4b. Both localized electromagnetic fields provide a favorable physical domain for their coupling, and result in an effective optical field confinement.

Moreover, the SP-induced optical field confinement will strengthen the light-matter interaction and accelerate the decay process.[27] As a result, the radiative recombination was enhanced while the nonradiative recombination was suppressed, so the UV emission of ZnO can be enhanced. This ultrafast dynamics has been demonstrated in Ag SP coupled ZnO nanowire very recently.[42] The similar process for graphene/ZnO system has also been confirmed in our previous reported time-resolved photoluminescence experiment.[43] As compared the PL spectra under the same excitation of 160 kW/cm^2 in Figure 4c, the lasing intensity of the hybrid microcavity exhibits nearly 10-fold enhancement after monolayer graphene was covered on the bare ZnO microrod. A careful observation reveals the fwhm of the bare and the hybrid microcavity is about 0.08 and 0.06 nm respectively, indicating the narrowed spectral width of the hybrid microcavity relative to that of the bare one, also implying the improvement of the lasing quality after graphene covering.

It is noted that a series of experimental and theoretical researches have demonstrated the absorption and dispersion of graphene and revealed the corresponding π and $\pi+\sigma$ plasmons.[40,41,44−46] For example, both theoretical calculation by Despoja *et al.*[44] and experimental measurement by Eberlein *et al.*[46] demonstrated a pronounced electronic excitation band of graphene around 4.5 eV (~275 nm) and clearly pointed out the SP generation in UV region due to the oscillation of π electrons. In our case, the PL enhancement ratio corresponding to different excitation wavelength was carried out to confirm the coupling mechanism between graphene SP and ZnO UV emission. The inset in Figure 5 displays the PL intensity of the ZnO before and after graphene covering under the femtosecond (fs) laser excitation with the same power but different wavelengths (namely 350, 325, 300, and 275 nm). The graphene/ZnO hybrid microcavity presented much higher PL intensity than the bare ZnO did under all of

the UV excitation wavelengths. It is worth to note that different excitation wavelength displays different enhancement ratio. In Figure 5, the UV part of the spectrum of electronic excitation in graphene from ref 44 was enlarged, while the measured PL enhancement ratio *vs* excitation wavelength was also plotted. It can be seen that the experimental enhancement data (blue curve) is consistent with Despoja's calculation (black curve)[44] and Eberlein's experiment (red dots)[46] results. This demonstrates clearly the contribution of graphene SP to ZnO UV emission.

As indicated by previous reports,[18,26] among many efforts to improve the optical performance of the semiconductor micro/nanostructures, the hybrid plasmonic microcavities have been proposed to modulate the oscillation feedback, reduce the waveguide and/or mirror loss through the coupling between the metal SP modes and conventional optical cavity modes.[47,48] On the basis of the optical field confinement and WGM lasing enhancement observed above, graphene was further applied to the small cavity with single mode lasing shown in Figure 3. Here, the hybrid microcavity was constructed by transferring a piece of monolayer graphene on the submicron-sized ZnO rod, and the EDX analysis was performed to confirm the coverage state of graphene. Figure 6a shows the SEM image of the hybrid microcavity and its EDX elemental mapping images of C, Zn and O. The Zn element distribution just corresponds to the top-view section of the ZnO rod, while, clear signals of C and O are also observed in the same region. This indicates the overlap of graphene on the ZnO rod. It should be noted that C and O distribute in the whole mapping region besides the ZnO position. The C signal is from the graphene extended out on the substrate and the extra O comes from the quartz substrate.

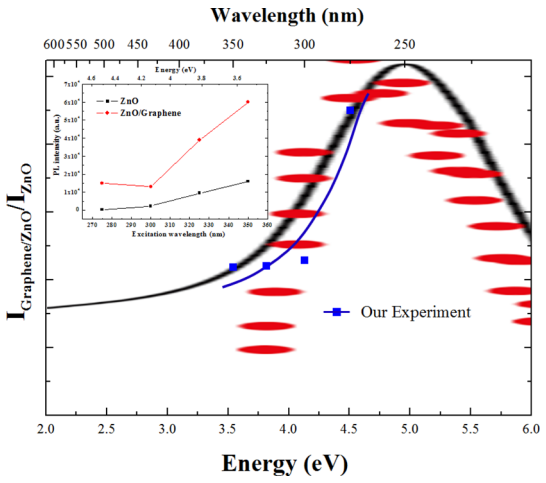

Figure 5. Comparison between the enlarged UV part of the spectrum of electronic excitation in graphene cited from ref 44 and the PL enhancement ratio of ZnO sample with graphene to without case. The black curve and red dots denotes Despoja's calculation (ref 44) and Eberlein's experiment (ref 46) result, respectively. The inset exhibits the PL intensity of the ZnO sample with and without graphene under fs laser excitation with the same power but different wavelength.

After graphene was covered on the submicron-sized ZnO rod, the lasing performance showed significant improvement, as shown in Figure 6b, which displays the excitation power density dependent PL spectra of the hybrid microcavity. Like that shown in Figure 3b, there is only one lasing peak appeared in the spectrum, but it is much stronger and sharper than that from the bare one. The lasing threshold of the hybrid microcavity is reduced from 800 to 600 kW/cm^2, while the fwhm of the lasing peak is reduced from 0.98 to 0.25 nm, and the *Q* factor is increased from 400 to 1500. The lasing peak intensity of the hybrid microcavity is about 4 times strong as that of the bare rod at the same excitation power density of 1000 kW/cm^2. This improvement of the lasing performance can be attributed to the coupling between the confined SP wave of graphene and the emission optical field of ZnO, as discussed above. As graphene was covered on the submicron-sized ZnO rod, the optical field was effectively confined in the hybrid cavity and the optical gain is highly improved due to the strong spatial confinement of the graphene SP.

CONCLUSION

In summary, single-mode UV lasing was realized in a submicron-sized ZnO rod based on the systematic

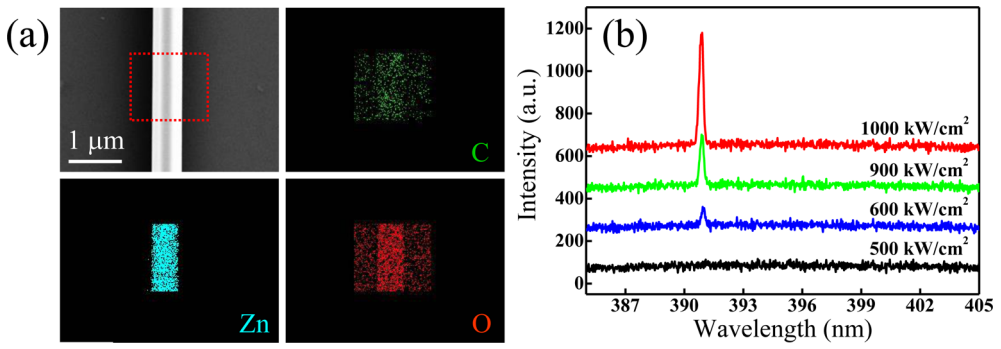

Figure 6. (a) SEM image of the graphene-coated submicron-sized ZnO rod and its EDX elemental mapping images of C, Zn and O in the red rectangular region. (b) PL spectra of this hybrid microcavity under different excitation power densities.

investigation of ZnO WGM lasing on dependence of the ZnO microrods diameters, and the lasing performance was remarkably improved by facilely covering a monolayer graphene on the submicron cavity. As graphene was covered on the rod to construct a graphene/ZnO hybrid microcavity in submicron scale, the optical field was effectively confined and the optical gain of the cavity was enhanced due to the coupling between graphene SP and the ZnO exciton emission. The graphene SP coupled ZnO lasing improvement technique may open new opportunities for practical applications of ZnO lasers, as well as providing new designs for realizing low-threshold single-mode lasers using other types of micro/nanostructures. The results also represent a significant technology in pursuit of ultrasmall lasers even breaking through the diffraction limit.

MATERIALS AND METHODS

The hexagonal ZnO microrods were synthesized by a vapor phase transport (VPT) method,[49] no catalyst, carrier gas, or vacuum condition was used in the experiment. Briefly, a mixture of high purity ZnO and graphite powders with definite mass ratio of 1:1 was filled into a quartz boat as source materials, and a cleaned silicon substrate was covered on the quartz boat. The boat was then placed in the center of a quartz tube and the whole assembly was put into a horizontal tube furnace. ZnO microrods with different diameters can be achieved by changing the temperature at range of 1000−1150 °C and the growing time ranging from 50 to 100 min. Then some microrods with different diameters were picked out and separately aligned on a quartz substrate to construct whispering-gallery microcavities. The monolayer graphene used in this experiment was synthesized by a chemical vapor deposition (CVD) method.[50] To explore the impact of graphene on the ZnO lasing performance, two kinds of microcavities were constructed for comparison, one is the bare ZnO microrod microcavity, the other is the graphene/ZnO hybrid microcavity, which was fabricated by transferring a piece of monolayer graphene on the same ZnO microrod.

The morphology of the bare and the hybrid microcavities were characterized by field emission scanning electron microscopy (FESEM, Carl Zeiss Ultra Plus), and the element mapping was carried out with the attached energy dispersive X-ray spectroscopy (EDX, Oxford X-Max 50). To measure the optical behaviors, the samples were excited by a 325 nm femtosecond (fs) laser (pulse duration of 150 fs, repetition rate of 1000 Hz) through a microphotoluminescence (μ-PL) system, where the excitation lasing was focused by a microscope objective (40×), the PL signals were collected by the same objective and recorded by a CCD detector. The data was collected by an optical multichannel analyzer (Princeton, Acton SP2500i). All measurements were performed at room temperature. Theoretical simulation was carried out using a finite difference time domain (FDTD) method by setting the refractive indexes as $n_{air} = 1.0$, $n_{ZnO} = 2.45$, and $\varepsilon = 5.28 + 7.78i$ for graphene according to previous reports.[51,52] Similar simulation has also been done in our previous report.[53]

Conflict of Interest: The authors declare no competing financial interest.

Acknowledgment. The authors would like to thank Prof. Zhenhua Ni and Dr. Haiyan Nan from Department of Physics, Southeast University for their warm help in the material synthesis. Dr. Mingming Jiang from State Key Laboratory of Luminescence and Applications, Changchun Institute of Optics, Fine Mechanics and Physics, Chinese Academy of Sciences was also acknowledged for the theoretical simulation. This work is supported by "973" Program (2011CB302004 and 2013CB932903), NSFC (61275054, 61475035, 11404289 and 11404328) and Open Research Fund of SEU-JGRI Joint Research Center of Advanced Carbon Materials.

REFERENCES AND NOTES

1. Klingshirn, C. ZnO: From Basics Towards Applications. *Phys. Status Solidi B* **2007**, *244*, 3027–3073.
2. Soci, C.; Zhang, A.; Xiang, B.; Dayeh, S. A.; Aplin, D. P. R.; Park, J.; Bao, X. Y.; Lo, Y. H.; Wang, D. ZnO Nanowire UV Photodetectors with High Internal Gain. *Nano Lett.* **2007**, *7*, 1003–1009.
3. Chu, S.; Wang, G. P.; Zhou, W. H.; Lin, Y. Q.; Chernyak, L.; Zhao, J. Z.; Kong, J. Y.; Li, L.; Ren, J. J.; Liu, J. L. Electrically Pumped Waveguide Lasing from ZnO Nanowires. *Nat. Nanotechnol.* **2011**, *6*, 506–510.
4. Cao, H.; Zhao, Y. G.; Ho, S. T.; Seelig, E. W.; Wang, Q. H.; Chang, R. P. H. Random Laser Action in Semiconductor Powder. *Phys. Rev. Lett.* **1999**, *82*, 2278–2281.
5. Huang, M. H.; Mao, S.; Feick, H.; Yan, H. Q.; Wu, Y. Y.; Kind, H.; Weber, E.; Russo, R.; Yang, P. D. Room-Temperature Ultraviolet Nanowire Nanolasers. *Science* **2001**, *292*, 1897–1899.
6. Czekalla, C.; Sturm, C.; Schmidt-Grund, R. d.; Cao, B.; Lorenz, M.; Grundmann, M. Whispering Gallery Mode Lasing in Zinc Oxide Microwires. *Appl. Phys. Lett.* **2008**, *92*, 241102.
7. Dai, J.; Xu, C. X.; Zheng, K.; Lv, C. G.; Cui, Y. P. Whispering Gallery-Mode Lasing in ZnO Microrods at Room Temperature. *Appl. Phys. Lett.* **2009**, *95*, 241110.
8. Nobis, T.; Rahm, A.; Czekalla, C.; Lorenz, M.; Grundmann, M. Optical Whispering Gallery Modes in Dodecagonal Zinc Oxide Microcrystals. *Superlattices Microstruct.* **2007**, *42*, 333–336.
9. Chen, R.; Ling, B.; Sun, X. W.; Sun, H. D. Room Temperature Excitonic Whispering Gallery Mode Lasing from High-Quality Hexagonal ZnO Microdisks. *Adv. Mater.* **2011**, *23*, 2199–2204.
10. Tu, X.; Wu, X.; Li, M.; Liu, L.; Xu, L. Ultraviolet Single-Frequency Coupled Optofluidic Ring Resonator Dye Laser. *Opt. Express* **2012**, *20*, 19996–20001.
11. Kalusniak, S.; Sadofev, S.; Halm, S.; Henneberger, F. Vertical Cavity Surface Emitting Laser Action of an All Monolithic ZnO-Based Microcavity. *Appl. Phys. Lett.* **2011**, *98*, 011101.
12. Nesnidal, M. P.; Mawst, L. J.; Bhattacharya, A.; Botez, D.; DiMarco, L.; Connolly, J. C.; Abeles, J. H. Single-Frequency, Single-Spatial-Mode Row-DFB Diode Laser Arrays. *IEEE Photonics Technol. Lett.* **1996**, *8*, 182–184.
13. Chen, L.; Towe, E. Nanowire Lasers with Distributed-Bragg-Reflector Mirrors. *Appl. Phys. Lett.* **2006**, *89*, 053125.
14. Wu, X.; Li, H.; Liu, L.; Xu, L. Unidirectional Single-Frequency Lasing from a Ring-Spiral Coupled Microcavity Laser. *Appl. Phys. Lett.* **2008**, *93*, 081105.
15. Wu, X.; Sun, Y.; Suter, J. D.; Fan, X. Single Mode Coupled Optofluidic Ring Resonator Dye Lasers. *Appl. Phys. Lett.* **2009**, *94*, 241109.
16. Xu, E.; Zhang, X.; Zhou, L.; Zhang, Y.; Yu, Y.; Li, X.; Huang, D. Ultrahigh-Q Microwave Photonic Filter with Vernier Effect and Wavelength Conversion in a Cascaded Pair of Active Loops. *Opt. Lett.* **2010**, *35*, 1242–1244.
17. Shang, L.; Liu, L.; Xu, L. Single-Frequency Coupled Asymmetric Microcavity Laser. *Opt. Lett.* **2008**, *33*, 1150–1152.
18. Li, K. H.; Ma, Z.; Choi, H. W. Single-Mode Whispering Gallery Lasing from Metal-Clad Gan Nanopillars. *Opt. Lett.* **2012**, *37*, 374–376.
19. Gargas, D. J.; Moore, M. C.; Ni, A.; Chang, S. W.; Zhang, Z. Y.; Chuang, S. L.; Yang, P. D. Whispering Gallery Mode Lasing from Zinc Oxide Hexagonal Nanodisks. *ACS Nano* **2010**, *4*, 3270–3276.
20. Lu, C.-Y.; Chang, S.-W.; Chuang, S. L.; Germann, T. D.; Bimberg, D. Metal-Cavity Surface-Emitting Microlaser at Room Temperature. *Appl. Phys. Lett.* **2010**, *96*, 251101.

21. Shi, X.; Wang, Y.; Wang, Z.; Sun, Y.; Liu, D.; Zhang, Y.; Li, Q.; Shi, J. High Performance Plasmonic Random Laser Based on Nanogaps in Bimetallic Porous Nanowires. *Appl. Phys. Lett.* **2013**, *103*, 023504.
22. Yu, K.; Lakhani, A.; Wu, M. C. Subwavelength Metal-Optic Semiconductor Nanopatch Lasers. *Opt. Express* **2010**, *18*, 8790–8799.
23. Perahia, R.; Alegre, T. P. M.; Safavi-Naeini, A. H.; Painter, O. Surface-Plasmon Mode Hybridization in Subwavelength Microdisk Lasers. *Appl. Phys. Lett.* **2009**, *95*, 201114.
24. Lim, K. P.; Lee, C. W.; Singh, G.; Wang, Q. Design of Ultrasmall Plasmonic Coaxial Lasers on Si. *J. Nanophotonics* **2013**, *7*, 070598.
25. Lee, C.-W.; Singh, G.; Wang, Q. Light Extraction - a Practical Consideration for a Plasmonic Nano-Ring Laser. *Nanoscale* **2013**, *5*, 10835–10838.
26. Oulton, R. F.; Sorger, V. J.; Zentgraf, T.; Ma, R. M.; Gladden, C.; Dai, L.; Bartal, G.; Zhang, X. Plasmon Lasers at Deep Subwavelength Scale. *Nature* **2009**, *461*, 629–632.
27. Koppens, F. H. L.; Chang, D. E.; de Abajo, F. J. G. Graphene Plasmonics: A Platform for Strong Light-Matter Interactions. *Nano Lett.* **2011**, *11*, 3370–3377.
28. West, P. R.; Ishii, S.; Naik, G. V.; Emani, N. K.; Shalaev, V. M.; Boltasseva, A. Searching for Better Plasmonic Materials. *Laser Photonics Rev.* **2010**, *4*, 795–808.
29. Liu, M.; Yin, X.; Ulin-Avila, E.; Geng, B.; Zentgraf, T.; Ju, L.; Wang, F.; Zhang, X. A Graphene-Based Broadband Optical Modulator. *Nature* **2011**, *474*, 64–67.
30. Chen, P.-Y.; Alu, A. Atomically Thin Surface Cloak Using Graphene Monolayers. *ACS Nano* **2011**, *5*, 5855–5863.
31. Gu, T.; Petrone, N.; McMillan, J. F.; van der Zande, A.; Yu, M.; Lo, G. Q.; Kwong, D. L.; Hone, J.; Wong, C. W. Regenerative Oscillation and Four-Wave Mixing in Graphene Optoelectronics. *Nat. Photonics* **2012**, *6*, 554–559.
32. Engel, M.; Steiner, M.; Lombardo, A.; Ferrari, A. C.; Loehneysen, H. V.; Avouris, P.; Krupke, R. Light-Matter Interaction in a Microcavity-Controlled Graphene Transistor. *Nat. Commun.* **2012**, *3*, 906.
33. Hwang, S. W.; Shin, D. H.; Kim, C. O.; Hong, S. H.; Kim, M. C.; Kim, J.; Lim, K. Y.; Kim, S.; Choi, S.-H.; Ahn, K. J.; *et al.* Plasmon-Enhanced Ultraviolet Photoluminescence from Hybrid Structures of Graphene/ZnO Films. *Phys. Rev. Lett.* **2010**, *105*, 127403.
34. Cheng, S. H.; Yeh, Y. C.; Lu, M. L.; Chen, C. W.; Chen, Y. F. Enhancement of Laser Action in ZnO Nanorods Assisted by Surface Plasmon Resonance of Reduced Graphene Oxide Nanoflakes. *Opt. Express* **2012**, *20*, A799–A805.
35. Kim, K.; Lee, S. M.; Do, Y. S.; Ahn, S. I.; Choi, K. C. Enhanced Photoluminescence from Zinc Oxide by Plasmonic Resonance of Reduced Graphene Oxide. *J. Appl. Phys.* **2013**, *114*, 074903.
36. Yang, W.; Hu, X. Comment on "Plasmon-Enhanced Ultraviolet Photoluminescence from Hybrid Structures of Graphene/ZnO Films. *Phys. Rev. Lett.* **2011**, *107*, 159701.
37. Dai, J.; Xu, C. X.; Xu, X. Y.; Guo, J. Y.; Li, J. T.; Zhu, G. Y.; Lin, Y. Single ZnO Microrod Ultraviolet Photodetector with High Photocurrent Gain. *ACS Appl. Mater. Interfaces* **2013**, *5*, 9344–9348.
38. Chen, R.; Sun, H. D.; Wang, T.; Hui, K. N.; Choi, H. W. Optically Pumped Ultraviolet Lasing from Nitride Nanopillars at Room Temperature. *Appl. Phys. Lett.* **2010**, *96*, 241101.
39. Saxena, D.; Mokkapati, S.; Parkinson, P.; Jiang, N.; Gao, Q.; Tan, H. H.; Jagadish, C. Optically Pumped Room-Temperature Gaas Nanowire Lasers. *Nat. Photonics* **2013**, *7*, 963–968.
40. Nair, R. R.; Blake, P.; Grigorenko, A. N.; Novoselov, K. S.; Booth, T. J.; Stauber, T.; Peres, N. M. R.; Geim, A. K. Fine Structure Constant Defines Visual Transparency of Graphene. *Science* **2008**, *320*, 1308–1308.
41. Sun, Z.; Yan, Z.; Yao, J.; Beitler, E.; Zhu, Y.; Tour, J. M. Growth of Graphene from Solid Carbon Sources. *Nature* **2010**, *468*, 549–552.
42. Sidiropoulos, T. P. H.; Roeder, R.; Geburt, S.; Hess, O.; Maier, S. A.; Ronning, C.; Oulton, R. F. Ultrafast Plasmonic Nanowire Lasers near the Surface Plasmon Frequency. *Nat. Phys.* **2014**, *10*, 870–876.
43. Li, J. T.; Xu, C. X.; Nan, H. Y.; Jiang, M. M.; Gao, G. Y.; Lin, Y.; Dai, J.; Zhu, G. Y.; Ni, Z. H.; Wang, S. F.; *et al.* Graphene Surface Plasmon Induced Optical Field Confinement and Lasing Enhancement in ZnO Whispering-Gallery Microcavity. *ACS Appl. Mater. Interfaces* **2014**, *6*, 10469–10475.
44. Despoja, V.; Novko, D.; Dekanić, K.; Šunjić, M.; Marušić, L. Two-Dimensional and Π Plasmon Spectra in Pristine and Doped Graphene. *Phys. Rev. B: Condens. Matter Mater. Phys.* **2013**, *87*, 075447.
45. Jovanović, V. B.; Radović, I.; Borka, D.; Mišković, Z. L. High-Energy Plasmon Spectroscopy of Freestanding Multilayer Graphene. *Phys. Rev. B: Condens. Matter Mater. Phys.* **2011**, *84*, 155416.
46. Eberlein, T.; Bangert, U.; Nair, R. R.; Jones, R.; Gass, M.; Bleloch, A. L.; Novoselov, K. S.; Geim, A.; Briddon, P. R. Plasmon Spectroscopy of Free-Standing Graphene Films. *Phys. Rev. B: Condens. Matter Mater. Phys.* **2008**, *77*, 233406.
47. Chang, S. W.; Lin, T. R.; Chuang, S. L. Theory of Plasmonic Fabry-Perot Nanolasers. *Opt. Express* **2010**, *18*, 15039–15053.
48. Jiang, M.-M.; Zhao, B.; Chen, H.-Y.; Zhao, D.-X.; Shan, C.-X.; Shen, D.-Z. Plasmon-Enhanced Ultraviolet Photoluminescence from the Hybrid Plasmonic Fabry-Perot Microcavity of Ag/ZnO Microwires. *Nanoscale* **2014**, *6*, 1354–1361.
49. Dai, J.; Xu, C. X.; Sun, X. W. ZnO-Microrod/p-GaN Heterostructured Whispering-Gallery-Mode Microlaser Diodes. *Adv. Mater.* **2011**, *23*, 4115–4119.
50. Li, X.; Cai, W.; An, J.; Kim, S.; Nah, J.; Yang, D.; Piner, R.; Velamakanni, A.; Jung, I.; Tutuc, E.; *et al.* Large-Area Synthesis of High-Quality and Uniform Graphene Films on Copper Foils. *Science* **2009**, *324*, 1312–1314.
51. Santoso, I.; Singh, R. S.; Gogoi, P. K.; Asmara, T. C.; Wei, D. C.; Chen, W.; Wee, A. T. S.; Pereira, V. M.; Rusydi, A. Tunable Optical Absorption and Interactions in Graphene *via* Oxygen Plasma. *Phys. Rev. B: Condens. Matter Mater. Phys.* **2014**, *89*, 075134.
52. Yang, L.; Deslippe, J.; Park, C. H.; Cohen, M. L.; Louie, S. G. Excitonic Effects on the Optical Response of Graphene and Bilayer Graphene. *Phys. Rev. Lett.* **2009**, *103*, 186802.
53. Jiang, M. M.; Li, J. T.; Xu, C. X.; Wang, S. P.; Shan, C. X.; Xuan, B.; Ning, Y. Q.; Shen, D. Z. Graphene Induced High-Q Hybridized Plasmonic Whispering Gallery Mode Microcavities. *Opt. Express* **2014**, *22*, 23836–23850.